



HAL
open science

Budyko framework based analysis of the effect of climate change on watershed characteristics and their impact on discharge over Europe

Julie Collignan, Jan Polcher, Sophie Bastin, Pere Quintana-Seguí

► To cite this version:

Julie Collignan, Jan Polcher, Sophie Bastin, Pere Quintana-Seguí. Budyko framework based analysis of the effect of climate change on watershed characteristics and their impact on discharge over Europe. 2022. insu-03892710v1

HAL Id: insu-03892710

<https://insu.hal.science/insu-03892710v1>

Preprint submitted on 10 Dec 2022 (v1), last revised 17 Oct 2023 (v2)

HAL is a multi-disciplinary open access archive for the deposit and dissemination of scientific research documents, whether they are published or not. The documents may come from teaching and research institutions in France or abroad, or from public or private research centers.

L'archive ouverte pluridisciplinaire **HAL**, est destinée au dépôt et à la diffusion de documents scientifiques de niveau recherche, publiés ou non, émanant des établissements d'enseignement et de recherche français ou étrangers, des laboratoires publics ou privés.

Budyko framework based analysis of the effect of climate change on watershed characteristics and their impact on discharge over Europe

Julie Collignan¹, Jan Polcher², Sophie Bastin³, and Pere Quintana-Seguí⁴

¹Laboratoire de Météorologie Dynamique/IPSL - Ecole Polytechnique/CNRS

²Laboratoire de Météorologie Dynamique (CNRS)/IPSL

³IPSL/LATMOS

⁴Observatori de l'Ebre (Universitat Ramon Llull - CSIC)

December 7, 2022

Abstract

In a context of climate change, the stakes surrounding water availability are getting higher. Decomposing and quantifying the effects of climate on discharge allows to better understand their impact on water resources. We propose a methodology to separate the effect of change in annual mean of climate variables from the effect of intra-annual distribution of precipitations. It combines the Budyko framework with outputs from a Land Surface Model (LSM). The LSM is used to reproduce the behavior of 2134 reconstructed watersheds over Europe between 1902 and 2010, with climate inputs as the only source of change. We fit to the LSM outputs a one parameter approximation to the Budyko framework. It accounts for the evolution of annual mean in precipitation (P) and potential evapotranspiration (PET). We introduce a time-varying parameter in the equation which represents the effect of long-term variations in the intra-annual distribution of P and PET. To better assess the effects of changes in annual means or in intra-annual distribution of P, we construct synthetic forcings fixing one or the other. The results over Europe show that the changes in discharge due to climate are dominated by the trends in the annual averages of P. The second main climate driver is PET, except over the Mediterranean area where changes in intra-annual variations of P have a higher impact on discharge than trends in PET. Therefore the effects of changes in intra-annual distribution of climate variables are not to be neglected when looking at changes in annual discharge.

1 **Budyko framework based analysis of the effect of**
2 **climate change on watershed characteristics and their**
3 **impact on discharge over Europe**

4 **Julie Collignan¹, Jan Polcher¹, Sophie Bastin², Pere Quintana-Segui³**

5 ¹Laboratoire de Météorologie Dynamique/IPSL - Ecole Polytechnique/CNRS -, Paris, France

6 ²Laboratoire Atmosphères, Observations Spatiales/IPSL - CNRS -, Paris, France

7 ³Observatori de l'Ebre (Universitat Ramon Llull – CSIC), Roquetes, Spain

8 **Key Points:**

- 9 • Evaluate the role of climate change on the evolution of discharge of European rivers.
- 10 • Using the Budyko model as a detection tool for changes in hydrological behaviors
- 11 of watersheds.
- 12 • Analyse the effects of changes in the intra-annual distribution of precipitations on
- 13 the evolution of the annual discharge.

Corresponding author: Julie Collignan, julie.collignan@lmd.ipsl.fr

14 Abstract

15 In a context of climate change, the stakes surrounding water availability are get-
 16 ting higher. Decomposing and quantifying the effects of climate on discharge allows to
 17 better understand their impact on water resources. We propose a methodology to sep-
 18 arate the effect of change in annual mean of climate variables from the effect of intra-
 19 annual distribution of precipitations. It combines the Budyko framework with outputs
 20 from a Land Surface Model (LSM). The LSM is used to reproduces the behavior of 2134
 21 reconstructed watersheds over Europe between 1902 and 2010, with climate inputs as
 22 the only source of change. We fit to the LSM outputs a one parameter approximation
 23 to the Budyko framework. It accounts for the evolution of annual mean in precipitation
 24 (P) and potential evapotranspiration (PET). We introduce a time-varying parameter
 25 in the equation which represents the effect of long-term variations in the intra-annual
 26 distribution of P and PET . To better assess the effects of changes in annual means or
 27 in intra-annual distribution of P , we construct synthetic forcings fixing one or the other.
 28 The results over Europe show that the changes in discharge due to climate are dominated
 29 by the trends in the annual averages of P . The second main climate driver is PET , ex-
 30 cept over the Mediterranean area where changes in intra-annual variations of P have a
 31 higher impact on discharge than trends in PET . Therefore the effects of changes in intra-
 32 annual distribution of climate variables are not to be neglected when looking at changes
 33 in annual discharge.

34 Plain Language Summary

35 Water availability is a high stake for all societies. Different competing activities rely
 36 on that resource and its scarcity challenges social, economical and environmental con-
 37 flicts. With climate change, river discharge and more generally the full water cycle is im-
 38 pacted. Furthermore, many human activities such as dams and irrigation concurrently
 39 change the balance of the water cycle over watersheds. Which is the impact of climate
 40 change on discharge? How to separate the effect of climate change from the effect of di-
 41 rect human activities? Models are a way to represent reality with an understanding of
 42 the physical phenomena included. They can be used to represent the behavior of water-
 43 sheds without human intervention. We develop a methodology to highlight the climate
 44 factors impacting discharge. It compares the impact of changes in seasonality to changes
 45 in annual averages of climate variables. We find that annual discharge changes are mostly
 46 driven by changes in annual precipitation over Europe. The increasing temperature leads
 47 to increasing evaporative demand and is the second most impacting factor over most of
 48 Europe. However, over the Mediterranean area where water is more limiting, changes
 49 in the seasonality of precipitations has a higher impact than changes in the evaporative
 50 demand.

51 1 Introduction

52 Water is a key resources for all societies and both its excess and its scarcity can
 53 lead to challenging economical, environmental and social issues. Understanding the hy-
 54 drological cycle and how it evolves due to a changing climate is a major challenge of the
 55 century. If we focus our analysis on past changes over Europe, the atmospheric demand
 56 for moisture (PET) has been raising, along with modifications of precipitations (P). The
 57 observed changes in P show that not only the annual average of P is changing but there
 58 are differences in these changes between Summer and Winter, dependent on the area (Zveryaev,
 59 2004). Over Europe, Christidis and Stott (2022) showed that the Mediterranean area
 60 tends to become dryer while the rest of Europe becomes wetter over the past century,
 61 with weaker relative trends in Summer than in Winter. Therefore it is important to not
 62 only look at the effects of changes in the annual averages of climate variables but also
 63 to look at the effect of changes in seasonality and intra-annual distribution of these vari-

64 ables. The distribution of P within the year and its coupling or decoupling from the at-
65 mospheric demand PET will influence the partitioning of water between evapotranspi-
66 ration and runoff at the annual scale.

67 Changes in the different climate variables governing the water cycle will evidently
68 change equilibriums in the water balance over the different watersheds, impacting the
69 discharge of rivers. Milly et al. (2005) showed that streamflow trends world wide are and
70 will continue to be significantly impacted by changes in climatic factors. Studies show
71 the impact of distribution and concentration of rainfall events on peaks of discharge Q
72 (Tuel et al., 2022). However rivers are also highly managed and human activities are a
73 main driver of change in the functioning of watersheds. The main difficulty in analyz-
74 ing the effect of climate is to decompose the effects of the different drivers of change on
75 discharge and isolate the effect of climate to better understand its relative importance.
76 Our goal in this study is to propose a tool which can decompose and analyze the sen-
77 sitivity of discharge to climate change and separate it from internal watershed changes.

78 Physical based hydrological and Land Surface Models (LSM) are getting more and
79 more complex, able to reproduce the behavior of watersheds and to model discharge. How-
80 ever due to that complexity, it is more difficult to decompose the effects of individual
81 climate factors and to interpret their outputs. Other types of models are simpler, de-
82 pendent on fewer variables, such as statistical models. These later models are more em-
83 pirical and their elaboration is often limited by the available data. They can't always
84 relate to physical phenomena due to their simplicity. Our methodology combines both
85 types of models to benefit from both the performance and complexity of the physical based
86 model and from the simplicity of analysis of the more empirical model.

87 The empirical framework we chose to work with is the Budyko framework. It is well-
88 known and widely used in hydrological studies. It relies on the annual mean of the wa-
89 ter and energy balance at the scale of a watershed (Tian et al., 2018), taking into account
90 the water and energy limitations of the physical system. This framework relies on the
91 hypothesis that each watershed is at an equilibrium and introduces an empirical param-
92 eter which encompasses the watershed characteristics and its evaporation efficiency. The
93 main limitation is that the empirical parameter fitted on discharge observations doesn't
94 distinguish between the concurring effects of climate change and human activities. Fur-
95 thermore these effects tend to change the annual evaporation dynamics of watersheds
96 and the equilibrium of the system on which the framework relies. The present study in-
97 troduces a time-moving window to fit the Budyko framework to better capture the ef-
98 fect of climate change and this transition of the equilibrium state.

99 To focus on the effects of climate change, the present study applies the Budyko frame-
100 work to outputs of a state of the art LSM. The LSM represents the physical behavior
101 of watersheds and the only source of change introduced in the dynamics of the modeled
102 watersheds is the evolving climate variables applied to the models. The use of LSM out-
103 puts also allows to play with the climate parameters to better separate the effects of the
104 different elements of climate change (changes in annual averages against changes in intra-
105 annual distribution of climate variables).

106 This article is structured as follows: we first present the Budyko framework with
107 its underlying hypothesis and limits. Then we explain the methodology we developed
108 to apply it to the chosen LSM. Synthetic forcings are created to test if our methodol-
109 ogy allows to analyse the effects of different aspects of climate change. We explain the
110 use of the time-moving window to look at temporal trends in the different climatic ef-
111 fects. Finally we explain the results obtained over Europe of the effect on discharge trends
112 over the past century of the different element of climate change (changes in annual av-
113 erages against changes in intra-annual distribution of climate variables).

2 The Budyko framework

2.1 General presentation

Over watersheds which can be considered as closed systems, the water balance equation (1) applies to explain the equilibrium between the variables of the hydrological cycle: the river discharge (Q), the evapotranspiration (E), the precipitation (P) and the change in the water storage over the watershed between two time steps (ΔS).

$$P - \Delta S = Q + E \quad (1)$$

Long-term, ΔS can be reasonably considered as negligible. Ideally, this hypothesis should be applied over a period long enough that the equilibrium of the system is reached (L. Zhang et al., 2008). This also supposes no external perturbations impacting the water budget such as groundwater mining or water transfers to or from other basins.

This hypothesis can be applied over time series of yearly resolution (hydrological year) or coarser, so we can be freed from seasonal variations of the water storage. For the region considered, the hydrological year starts in September, at the end of the dry season, when the reservoirs are supposedly filled at their lowest, to minimize the differences in ΔS from one year to another. Later on, unless specified otherwise, the variables P , E and Q represent the annual averages over the hydrological year.

Commonly used in hydrological research to study Q and E , the Budyko framework relies on this long-term equilibrium of water balance over a catchment, coupled to the energy balance. It postulates that the partition of annual water budget between runoff and evapotranspiration over a catchment, represented by the evapotranspiration E , is a function of the relative water supply (rainfall P) and the atmospheric water demand (potential evapotranspiration PET) (Tian et al., 2018; Xing et al., 2018; Yang et al., 2007). The later depends on both the energy availability and on atmospheric turbulences. Therefore this framework takes into account the water and energy limitations of the system which can't evaporate more than the atmospheric demand allows and more water than the catchment reaches with the source of water (P). Different analytical approximations to this hypothesis (Budyko curves) have been developed, expressing the evapotranspiration rate (E/P) as a function of the aridity index (PET/P) over a catchment (fig. 1).

This framework relies on a closed water budget in time and space and neglects ΔS . So it has to be applied over a closed watershed and fitted on a long-term equilibrium. Therefore it is applied over annual averages at the very least and adjusted over several years to consider a long-term equilibrium and validate the hypothesis on ΔS .

2.2 One parameter equation

Parametric equations were developed, introducing an empirical parameter representing the catchment characteristics. Two of the most widely used are the Fu's equation (2) (Ning et al., 2019; Simons et al., 2020; L. Zhang et al., 2008; Zheng et al., 2018) and the Mezentsev–Choudhury–Yang equation (3) (Luo et al., 2020; Roderick & Farquhar, 2011; Wang et al., 2020; Xing et al., 2018; Xiong et al., 2020). These equations can be found under different names in the literature such as Tixeront-Fu equation for (2) or Turc-Mezentsev for (3) (Andréassian & Sari, 2019).

$$\frac{E}{P} = 1 + \frac{PET}{P} - \left(1 + \left(\frac{PET}{P} \right)^\nu \right)^{\frac{1}{\nu}} \quad (2)$$

$$E = \frac{P * PET}{(P^\omega + PET^\omega)^{\frac{1}{\omega}}} \quad (3)$$

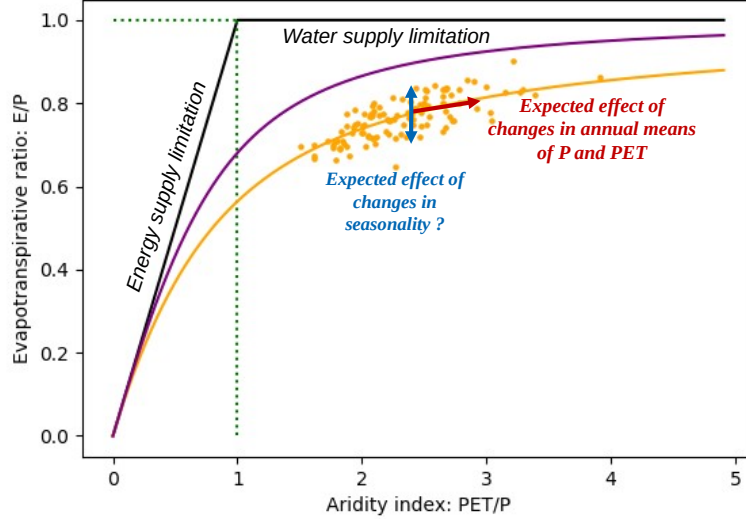


Figure 1. Budyko framework: relationship between evapotranspirative ratio (E/P) and aridity index (PET/P) (Fu’s equation). E , PET , P are annual averages. ν associated to the purple curve is larger than ν associated to the orange curve and translate in a higher evaporation efficiency above the watershed. For a given watershed with constant characteristics, there is still a dispersion around the curve of the dots for a given year due to intra-annual variations of the climate cycle (orange dots). The curve and its associated ν represents the average behavior of the watershed. The original framework includes trends in annual climate variables by a displacement along the curve (red arrow). However it doesn’t include trends which could impact the way water is partitioned over the catchment such as long-lasting trends in intra-annual distribution of P and PET (blue arrows).

157 The two parameters derived from equation (2) and (3) are linearly correlated, im-
 158 plying that both equations are almost equivalent (Andréassian & Sari, 2019; du et al.,
 159 2016; Roderick & Farquhar, 2011). We examine the sensitivity of the results to the para-
 160 metric equation used. A limitation exists when fitting Fu’s equation for watersheds with
 161 a particularly high dryness index such as in arid climates. In these areas, the uncertainty
 162 of the estimated ν will increase as the values used to fit the curve are all too close to the
 163 plateau (fig 1) and not scattered enough to correctly fit the curve. We fit the watershed
 164 parameter ω with Choudhury’s equation (3) and a set of E/PET and P/PET . This method
 165 ratios to PET gives us a plateau in humid areas as opposed to the previous fit ratioed
 166 to P . We obtain very similar results for the methodology with either equation used. We
 167 conclude that our area of study is not strongly impacted by this issue and that we could
 168 use either equation. For the rest of the study, we use results obtained with Fu’s equa-
 169 tion (2).

170 Evapotranspiration (E) measurements are not available over large spatial and tem-
 171 poral scales. Therefore most study work from discharge (Q) analysis. Q can be calcu-
 172 lated from the water balance equation (1) where ΔS has been neglected. With Fu’s equa-
 173 tion (2) used to express E in (1), it yields (4):

$$174 \quad Q = P * \left(1 + \left(\frac{PET}{P} \right)^\nu \right)^{\frac{1}{\nu}} - PET = f(P, PET, \nu) \quad (4)$$

175 2.3 Discussion of the watershed parameter

176 The watershed parameter is empirical, calculated by fitting the data over a specific
 177 catchment for a given time-period considered to be in an equilibrium state. It de-
 178 termines the shape of the curve. It reflects the various hydrological characteristics of the
 179 watershed such as topography, vegetation coverage, soil properties, etc, which play a part
 180 in the annual partitioning of water between evapotranspiration and runoff over the catch-
 181 ment.

182 The original Budyko hypothesis considers a stable equilibrium state of the water-
 183 shed behavior over the entire period studied. It correspond to a given curve (fig. 1) with
 184 a given value of the parameter ν for one watershed. The evolution of climate is taken
 185 into account through the evolution of annual averages of climate variables (fig. 1, red
 186 arrow). The variability of the annual values (E/P , PET/P) around the fitted curve are
 187 due to intra-annual variations of the climate cycle, such as the distribution of rain which
 188 changes the covariance between P and PET over the year. For instance, a difference in
 189 heavy rain events over a catchment can change the capacity of the soil to store water and
 190 change the dynamic of the water partition into runoff and evaporation even if the an-
 191 nual amount of precipitation stays constant. More generally, a change in synchroniza-
 192 tion between P (water available) and PET (energy demand from the atmosphere) will
 193 change E/P for the same average climate (Abatzoglou & Ficklin, 2017; S. Li et al., 2022).
 194 In an equilibrium state, the intra-annual variations are supposedly without trends and
 195 white noise around that equilibrium. The fitted parameter ν represents the average be-
 196 havior of the basin.

197 However watersheds are not always in an equilibrium state. In the various factors
 198 characterized with the watershed parameter ν , some can be considered as time invari-
 199 ant (soil type, topography, ...) while others are possibly affected by long-lasting changes.
 200 Then the original framework reaches a limit. Furthermore, changes can occur in the hy-
 201 drological properties of the surface water system, most likely due to direct human in-
 202 tervention such as river management, irrigation, land cover change, while other changes
 203 can occur due to climate change or to other climate land surface feedbacks, such as long-
 204 lasting changes in heavy raining events and seasonality of climate variables. One diffi-
 205 culty is that these changes are often simultaneous and the framework being semi-empirical,
 206 it does not allow to separate these types of changes easily.

207 Several studies attempt to address these deficiencies. Most studies consider a change
 208 between two periods considered as stable, a period of reference and a period post-changes
 209 (Jiang et al., 2015; Luo et al., 2020; Wang et al., 2020; Zhao et al., 2018; Zheng et al.,
 210 2018) and fit the parameter independently over each period. They obtain two different
 211 curves (fig. 1) with two different watershed parameter characterizing the two different
 212 equilibrium state before and after change. As a first hypothesis, they then consider that
 213 changes in the parameter are only due to anthropogenic changes. Assuming ν to be cli-
 214 mate invariant, the changes due to climate is taken into account in the framework only
 215 through the changes of the average P and PET (fig. 1, red arrow). Such method neglects
 216 the potential effects of climate, such as evolution of seasonality of climate variables, on
 217 the evolution of watersheds behaviors reflected by the watershed parameter (fig. 1, blue
 218 arrows).

219 In a second type of attempt, several studies developed an expression of the water-
 220 shed parameter as a function of significant factors. This would allow to express the evo-
 221 lution of ν over time and decompose the effects of climate and human activities through
 222 the different factors chosen. Different methods such as step-wise regressions, neural net-
 223 work were used to identify pertinent factors. However it requires to have enough infor-
 224 mation on the factors chosen and strong hypotheses stand behind the expression. Ning
 225 et al. (2019); Tian et al. (2018); D. Li et al. (2013); S. Li et al. (2022); Xing et al. (2018);
 226 X. Zhang et al. (2019), constructed their function across several basins, accounting for

227 spatially different human, climate and land characteristics. Environmental factors such
 228 as soil moisture, seasonality of P and PET , aridity index (S. Li et al., 2022; Ning et al.,
 229 2019), vegetation fraction and routing depth (Gentine et al., 2012; D. Li et al., 2013; Ning
 230 et al., 2019), relief ratio, drought severity index, seasonality of P and synchronicity be-
 231 tween P and PET (Xing et al., 2018) were selected depending on the study. Direct hu-
 232 man factors considered were irrigated area (Tian et al., 2018) or water applied for irri-
 233 gation (D. Li et al., 2013), land use and land cover change in highly managed areas (Tian
 234 et al., 2018) or even GDP per capita (X. Zhang et al., 2019). Other factors were tested
 235 but not selected, some selected in some studies but not in others, showing the high de-
 236 pendence of the final expression on the choice of factors tested and on the area of study.
 237 One strong hypothesis is then that such a relationship defined over spatial differences
 238 is also applicable to explain temporal differences (Luo et al., 2020).

239 Other studies (Jiang et al., 2015; Zhao et al., 2018) looked at time-varying human
 240 activities and climate change to construct expressions over time, using a time-moving
 241 window to fit the evolution of the catchment parameter over a basin. Factors chosen were
 242 temperature, PET and irrigated areas (Jiang et al., 2015). This approach faces another
 243 limitation due to the availability of information on the time evolution of the different fac-
 244 tors. Ning et al. (2019) used a mixed technique, applying their fit across 30 basins at dif-
 245 ferent time scales using moving time-windows and found that the impact of vegetation
 246 cover and climate seasonality on the watershed parameter was stronger over longer time
 247 steps.

248 3 Methodology

249 The methodology proposed here uses the Budyko framework to explore the sen-
 250 sitivity of discharge to climate change. It focuses on the parameter ν and attempts to
 251 decompose its dependence on climate. We want to explore the climate dependence of ν ,
 252 without having to express it directly. We use the output of a Land Surface Model to re-
 253 produce the behavior of watersheds with constant characteristics, subjected to climate
 254 change but no other source of change. We develop a time varying $\nu(t)$ to capture part
 255 of the change in the behavior of the watersheds due to climate. We compare its effects
 256 to the magnitude of change in discharge already captured with the traditional framework
 257 which only considers changes in annual averages of P and PET .

258 3.1 Simulations with a Land Surface Model (LSM)

259 To isolate the effect of climate change from other factors which could affect water-
 260 sheds, we work with outputs of a Land Surface Model (LSM). The model constructs wa-
 261 tersheds with constant hydrological properties and represents an idealized watershed, with-
 262 out any direct changes from human intervention and other non climatic perturbations.
 263 Therefore the only source of long-term change would be due to a difference in response
 264 to an evolving climate.

265 3.1.1 A "natural reference" simulation

266 In this study, we use the LSM Organizing Carbon and Hydrology In Dynamic Ecosys-
 267 tems (ORCHIDEE) from the Institut Pierre Simon Laplace (IPSL). It includes biophys-
 268 ical and biogeochemical processes to simulate the global carbon cycle and quantify ter-
 269 restrial water and energy balance. It can be run coupled to an atmospheric model or in
 270 off-line mode. In that latter case, the atmospheric conditions are forced by an independ-
 271 ent dataset. In the following, we will use the model in stand-alone conditions, with the
 272 forcing dataset GSWP3 which covers 1901 to 2013 (Hyungjun, 2017) with a resolution
 273 of 0.5° for all climate variables. The hydrological network of the ORCHIDEE LSM is con-
 274 structed from the hydrological elevation model HydroSHEDS (Lehner et al., 2008) which

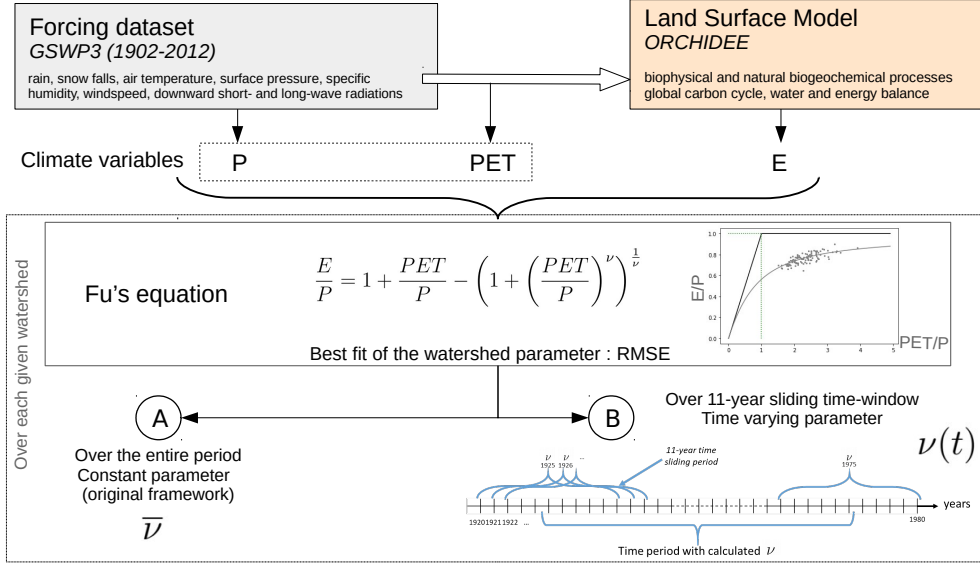


Figure 2. Scheme of the method: The Land Surface Model (LSM) is forced with the forcing dataset to calculate E . The LSM is considered to represent the "climatic reality" over a catchment, without any changes in the watershed characteristics. We then average P , PET and E and integrate it over each watershed to get annual averages for all catchments. Then we fit Fu's equation. A) The fit of the equation over the entire century results in the calculation of an empirical parameter $\bar{\nu}$ which represents the average catchment characteristics. B) To have an evolution of $\nu(t)$ over time, the fit was in a second time applied successively over an 11-year sliding time-period.

275 covers the area studied with the resolution of 30 arc seconds (approximately 1 kilome-
 276 ter at the equator). The hydrological information is then upscaled to the resolution of
 277 the atmospheric grid, the hydrological coherence being preserved by the construction of
 278 Hydrological Transfer Units (HTU) at the sub-grid level (Polcher et al., 2022). From a
 279 database of gauging stations, upstream basins are reconstituted on the hydrological ele-
 280 vation model grid and then projected on the atmospheric grid during the process. We
 281 have access to 2134 stations over the area studied for which the LSM calculates a dis-
 282 charge and for which we have the reconstituted upstream basin.

283 We consider that the final product correctly reproduces the hydrological network
 284 and the water partitioning over a watershed due to climatic phenomena. The modeled
 285 watersheds have fixed constant land surface characteristics which will react to the cli-
 286 mate data input at each time step (30 min time step). Therefore the LSM output de-
 287 pend on both the evolving annual average and the evolving distribution over the year
 288 of the climate variables.

289 The watershed parameter of the Budyko curve is calculated over each catchment
 290 with a fit of the equation curve $E/P = f(PET/P)$ (equation 2), using the minimum
 291 root mean square error (RMSE) for a given set of annual averages of evapotranspiration
 292 E , precipitation P and potential evapotranspiration PET data (Jiang et al., 2015; Yang
 293 et al., 2007).

294 The climatic variables defining P and PET are from a forcing dataset, GSWP3
 295 here. P is the sum of rainfall and snowfall. PET is calculated through Penman-Monteith

Table 1. Synthetic forcings created

	Forcing name	Average P	Intra-annual variation of P	Description ^a
1	<i>ref</i>	-	-	Reference forcing: GSWP3 (1901-2012)
2	<i>f2000</i>	fixed	fixed	<i>P</i> has been entirely fixed for each year, equal to the precipitation and the seasonality of the year 2000.
3	<i>cstmean</i>	fixed	-	Only the average value of <i>P</i> has been fixed for every year to the one of year 2000
4	<i>cstintravar</i>	-	fixed	Only the intra-annual variations of <i>P</i> have been fixed for every year to the one of year 2000

^aFor forcings 2 to 4, *P* has been modified compared to the reference: the average value of *P* over the year and/or the distribution of precipitations over the year have been fixed for each year to the value of the year 2000.

296 equation applied at a 30 min time step (Barella-Ortiz et al., 2013). *E* is the output of
 297 the LSM forced with the same forcing. The gridded outputs (*PET*, *E*) are at the res-
 298 olution of the forcing dataset (0.5°). Then we consider the annual mean *P*, *PET* and
 299 *E* over hydrological years, integrated over each catchment. The catchments' shape has
 300 been reproduced at finer resolution and then projected on the 0.5°grid.

301 We fit the parameter once with all points over the entire time period covered by
 302 the climate dataset to get $\bar{\nu}$ representing the average behavior for each catchment (fig.
 303 2, A).

304 **3.1.2 Synthetic forcings to analyze the effect of variation of seasonal-** 305 **ity**

306 In order to better understand the effect of inter and intra-annual climate variations
 307 on the Budyko framework and on discharge *Q*, we constructed synthetic climate forc-
 308 ings. To separate the effect of changes in annual averages of climate variables from the
 309 effect of changes in the intra-annual covariance of *P* and *PET*, we constructed synthetic
 310 forcings fixing one or the other.

311 The calculation of *PET* is based on Penman-Monteith equation applied at a 30 min
 312 time step (Barella-Ortiz et al., 2013). It includes many related climate variables and non-
 313 linear relationships, making it very difficult to anticipate how a change in a given climate
 314 variable may influence its behavior. It was therefore too complicated create synthetic
 315 forcings for which we would modify climate variables in order to fix *PET* seasonality for
 316 instance. Therefore we only modify the precipitation *P* in the synthetic forcings, to see
 317 how it impacts our results compared to the reference forcing.

318 The reference forcing is the GSWP3 dataset from September 1901 to September
 319 2012 (3h time step). Then we constructed three forcings which were modified over hy-
 320 drological years (table 1, fig. 3a):

- 321 • *f2000*: A forcing where all 3h values of *P* are set to the values of the year 2000
 322 (September 1999 to September 2000) for each year. Therefore all component of
 323 *P* (average and intra-annual variations) are set constant.

- 324 • *cstmean*: A forcing for which we keep the relative intra-annual distribution of P
325 of each year but where the average P of each year was set constant. The 3h val-
326 ues of P are scaled so the yearly average over the hydrological year is set to the
327 one of the year 2000 (September 1999 to September 2000).
- 328 • *cstintravar*: A forcing for which we keep the annual average of P for each year but
329 where the relative intra-annual distribution of P was set constant. The 3h values
330 of P are set to the values of the year 2000 (September 1999 to September 2000)
331 for each year and then scaled over each hydrological year so the yearly average is
332 set to the one of the corresponding year in the reference forcing.

333 Fig. 3a shows the resulting annual averages of P , PET , E integrated over a given
334 catchment in southern Spain, along with the average monthly distribution of P over the
335 year for each modified forcing. PET is the same for all forcings. The inter-annual vari-
336 ability of P and E is canceled for *f2000* since the variability of E over that area is mostly
337 linked to P . The inter-annual variability of E for *cstmean* is highly reduced but not com-
338 pletely canceled since it is also dependent on intra-annual distribution of P . For *ref* and
339 *cstintravar*, the average monthly distributions of P shown here are computed over the
340 century. It however varies from one year to another which is not illustrated here. For
341 *f2000* and *cstmean*, the average monthly distribution of P shown here corresponds to
342 the distribution of P over the year 2000 and is the same for each year in these forcings,
343 with just a scaling difference in the forcing *cstmean*. Over that given watershed, it re-
344 sults in a concentration of P over April and October and a particularly dry month of Febru-
345 ary over every year.

346 We expect that the Budyko framework will work better to reproduce the LSM out-
347 put when the variation of intra-annual distribution of P are canceled. Indeed the vari-
348 ability of the annual points (E/P , PET/P) around the curve (fig. 1) should be highly
349 reduced.

350 3.2 Introducing a time-varying watershed parameter ν

351 For a watershed with constant hydrological properties (which is the case when we
352 consider modeled watershed in ORCHIDEE), if we consider that ν is independent of cli-
353 mate, it should be time invariant.

354 However, the intra-annual synchronization of P and PET (or the annual covari-
355 ance between PET and P) impacts the annual mean of E and Q and the average effect
356 of this synchronization is included in the adjustment parameter ν , which is therefore not
357 completely independent of climate. Through its simple framework, the Budyko model
358 does not cover possible changes at intra-annual time scales which can impact the covari-
359 ance between PET and P over a year. Therefore long-term changes in seasonality should
360 induce a climatic time dependence, not accounted for in the framework with a constant
361 ν . Considering a time varying parameter should therefore improve the Budyko model
362 to better reproduce E and its climatic evolution.

363 3.2.1 Fit with a sliding time-window

364 To get a time varying parameter $\nu(t)$ for each catchment, we do several fits over
365 successive 11-year time-sliding sub-periods (fig. 2, B).

366 We chose 11 years as the smallest time-length over which we could apply the Budyko
367 framework relevantly, considering that each 11-year sub-period is stationary ($\Delta S = 0$).
368 Tian et al. (2018) found that below than time length the fit of the ν parameter was too
369 unstable to be relevant.

370 This time-varying $\nu(t)$ should enable to capture the possible long-term (above 10
371 years) variations in the intra-annual water-partitioning over a catchment. These long-

372 term changes in the annual covariance between P and PET should be the main climatic
 373 factors involved in the climatic dependence of ν . The variations of ν may however not
 374 be completely independent of the annual averages of P and PET . Crossed effects be-
 375 tween annual averages and intra-annual distributions would also be captured into ν vari-
 376 ations. For instance, a concentration of raining events over a shorter period would in-
 377 crease the runoff (change in intra-annual distribution of P), effect which would be am-
 378 plified by an increase of the total amount of water rained (change in annual average of
 379 P).

380 **3.2.2 Decomposing the impact of climate on discharge trends**

381 The watershed parameter ν is a conceptual variable providing little insight into the
 382 magnitude of discharge changes. We thus examine the impact of $\nu(t)$ changes on the river
 383 discharge Q and compare the impact of these changes to the impact of annual averages
 384 of climate variables (P and PET) changes on Q over time. We gather P and PET in
 385 a "climate" variable $C = (P, PET)$ to simplify the discussion.

386 Following our previous hypothesis (equation 4), Q can be estimated with the Budyko
 387 framework using C and ν : $Q = f(C, \nu(t))$.

388 Q can be decomposed with first order partial derivatives (equation 5), with the first
 389 term of the right hand side, representing the partial derivative due to climate variables
 390 C and the second term for the partial derivative due to changes in the watershed param-
 391 eter $\nu(t)$. We then estimate the partial derivatives due to C and due to ν independently.

$$392 \quad \frac{dQ}{dt} = \frac{\delta Q}{\delta C} \frac{dC}{dt} + \frac{\delta Q}{\delta \nu} \frac{d\nu}{dt} \quad \text{with } C = (P, PET) \quad (5)$$

393 To independently estimate the partial derivative due to climate variables C , we need
 394 to cancel the second term. To do so, we calculate the discharge $Q_c = f(C, \bar{\nu})$, with a
 395 constant value of ν . The trend of that discharge $\frac{dQ_c}{dt}$ matches the term with the partial
 396 derivative due to C in equation (5).

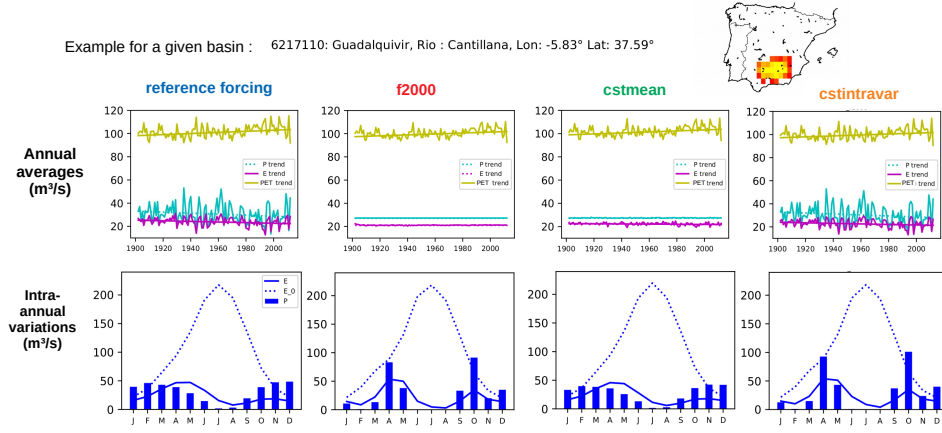
397 To estimate the partial discharge trend due to $\nu(t)$, we need eliminate the trends
 398 in annual averages of P and PET over the century to cancel the first term. We randomly
 399 draw P and PET pairings for each year. We do so several times and average the results
 400 for each year. It gives us a random climate without trends over the century. We then
 401 apply Fu's equation (2) with the resulting random annual averages of P and PET and
 402 the time varying $\nu(t)$ calculated with the forcing before the random drawing. It gives
 403 $Q_\nu = f(C_{rand}, \nu(t))$ for which the climate trends are only due to variations captured
 404 by the time varying parameter $\nu(t)$. The trend $\frac{dQ_\nu}{dt}$ matches the term with the partial
 405 derivative due to ν in equation (5). In the end, we get:

$$406 \quad \frac{dQ}{dt} = \frac{dQ_c}{dt} + \frac{dQ_\nu}{dt} \quad (6)$$

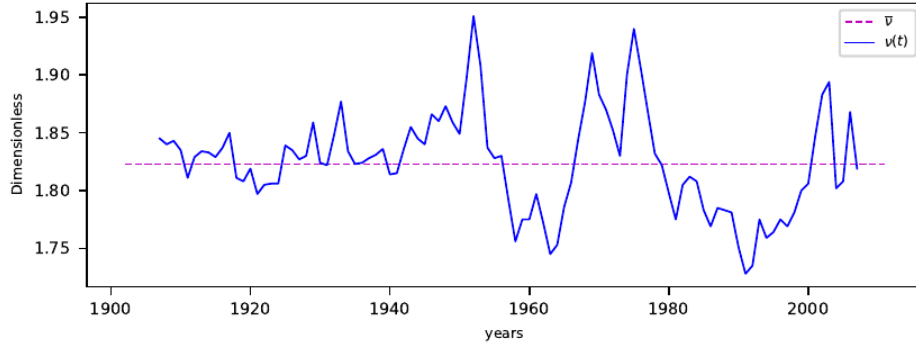
407 We calculate the trends of each term and their significance using the Mann-Kendall
 408 non-parametric test, associated to Thiel-Sen slope estimator.

409 This gives us time-series and associated trends for each of the watershed studied.
 410 Fig. 3 shows an example for a watershed in southern Spain. Fig. 3a shows the inter-annual
 411 variability of annual averages of climate variables P , PET directly calculated from the
 412 atmospheric forcing and E modeled by the LSM, for the different synthetic forcings. Over
 413 this watershed, E mostly relates to P . Fig. 3b shows the time-varying $\nu(t)$ resulting from
 414 the time-sliding window calculation (blue curve), compared to $\bar{\nu}$ calculated with one fit
 415 over the entire century (dashed purple line), for the reference forcing. The bottom plot

(a) Watershed. The colors show the share of the grid point within the watershed. Yellow points are completely within it while bordering grid points are red. Modified forcings over a given basin: the first row of graphs shows the inter-annual variability of P , PET and E for each forcings. The second row shows the average seasonal distribution of P over the catchment for each forcings over the entire century. The average monthly distributions of P shown here are computed over the century. It however varies from one year to another for the reference forcing and the forcing $cstmean$ which is not illustrated here.



(b) Watershed parameter $\bar{\nu}$ fitted over the entire time period (dashed purple line) and $\nu(t)$ fitted successively over a sliding 11-year time-window (blue line) for the reference forcing.



(c) Discharge estimated with Budyko for the reference forcing: $Q = f(P, PET, \nu(t))$ (blue line), $Q_c = f(P, PET, \bar{\nu})$ (purple line), $Q_\nu = f(P_{rand}, E_{0rand}, \nu(t))$ (black line) with their associated trends. Unsignificant trends are dashed. Here all trends are significant.

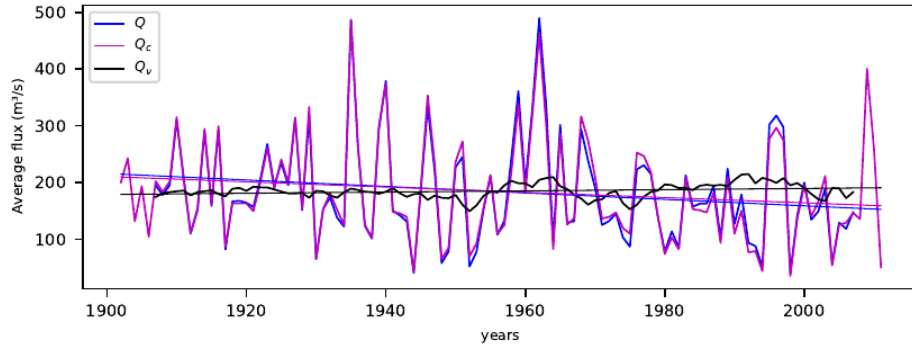


Figure 3. Time series obtained through the full application of our methodology for a given basin

416 in fig. 3c shows the decomposition of the discharge, comparing the full discharge to par-
 417 tial discharges and their respective trends. The full discharge Q is modeled with the Fu's
 418 equation with annual averages of P and PET from the reference forcing and $\nu(t)$. The
 419 first partial discharge Q_C is the one calculated without $\nu(t)$ variations. It covers most
 420 of Q variations for that given basins. The second partial discharge Q_ν covers some of
 421 the missing variations of Q and some of the missing trend. From that figure we can con-
 422 clude that most variations and trends of the discharge in this basin are explained by $C =$
 423 (P, PET) .

424 4 Results

425 4.1 Performance of Budyko with or without a time variant ν param- 426 eter

427 Our hypothesis is that for watershed with constant hydrological properties, the dis-
 428 persion of annual points around the curve is due to intra-annual variations of climate.
 429 If these variations did not exist, the original framework should be very close to perfect
 430 to model the discharge Q .

431 To test this hypothesis, we examine the performance of the original Budyko frame-
 432 work with a constant parameter $\bar{\nu}$ to reproduce the discharge from the LSM for the ref-
 433 erence forcing compared to the forcing *cstintravar*. For that later forcing, we removed
 434 the intra-annual variations of P from one year to another which should improve the per-
 435 formance of the Budyko framework close to perfect if the hypothesis is valid.

436 We use the Nash-Sutcliffe coefficient (NSC) as performance indicator (equation (7),
 437 fig. 4). We consider a $NSC > 0.5$ to be satisfactory (Moriasi et al., 2007).

$$438 \quad NSC = 1 - \frac{\sum_{i=0}^{years} (Ql_i - Qb_i)^2}{\sum_{i=0}^{years} (Ql_i - \bar{Q})^2} \left\{ \begin{array}{l} \text{with } Ql = \text{discharge from the LSM} \\ \text{and } Qb = \text{Result from the methodology with Fu's equation} \end{array} \right. \quad (7)$$

439 We obtain NSC values above 0.5 for 89.9% of all 2134 watershed tested for the orig-
 440 inal Budyko framework (Q_c , calculated with a constant ν) applied with the reference forc-
 441 ing (boxplot on the left, fig. 4). The original framework is therefore already effective to
 442 reproduce the annual discharge over watersheds with constant hydrological properties
 443 reacting to an evolving climate.

444 For the forcing *cstintravar*, NSC for Q_c increases to above 0.6 for all watersheds
 445 (boxplot on the right, fig. 4). This confirms our hypothesis: the framework is even more
 446 effective if there are no intra-annual variations of P from one year to another. Most of
 447 the variability not captured by the original framework is therefore due to the intra-annual
 448 variability of P and the covariance of P and PET .

449 When looking at NSC for the framework applied to the reference forcing with a time
 450 varying parameter $Q(ref) = f(C(ref), \nu(t))$, we gain up to 0.26 points of NSC for the
 451 tested watershed and reach 94.1% of all watersheds with $NSC > 0.5$ (boxplot on the cen-
 452 ter, fig. 4). It doesn't reach the performance of Q_c with the forcing *cstintravar* but en-
 453 ables to capture some of the variation due to intra-annual trends of climate variables.
 454 The part captured are long-term trends due to our choice of the 11-year time moving
 455 window. This validates our hypothesis that the introduction of a time varying watershed
 456 parameter $\nu(t)$ improves the framework to better encompass climate variability and the
 457 effect of climatic trends on discharge, including the effect of climate change on intra-annual
 458 distribution and covariance of climate variables (P and PET).

459 To sum up, most of the inaccuracy of the original framework for watershed with
 460 constant hydrological properties are due to variability in intra-annual distribution of cli-

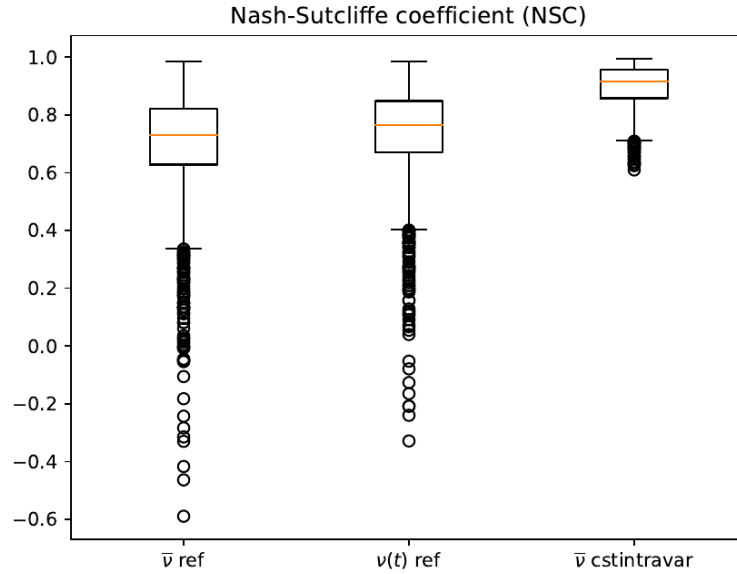


Figure 4. Boxplot of Nash-Sutcliffe coefficient (NSC) over all watersheds: for the forcing of reference with the constant parameter $\bar{\nu}$, with the time varying parameter ν and for the forcing *cstintravar* (where the seasonal distribution of P have been fixed over the entire time period) with a constant $\bar{\nu}$. It represents how well Budyko framework reproduces the discharge output from ORCHIDEE. A value above 0.5 is considered as satisfactory. Very similar results are found when looking at R^2 from a linear regression.

461 mate variables (P and PET). Our time varying parameter improves the framework by
 462 allowing to capture long-term trends in these variations. We now analyze their effect on
 463 discharge, compare to the effect of trends in annual average of climate variables.

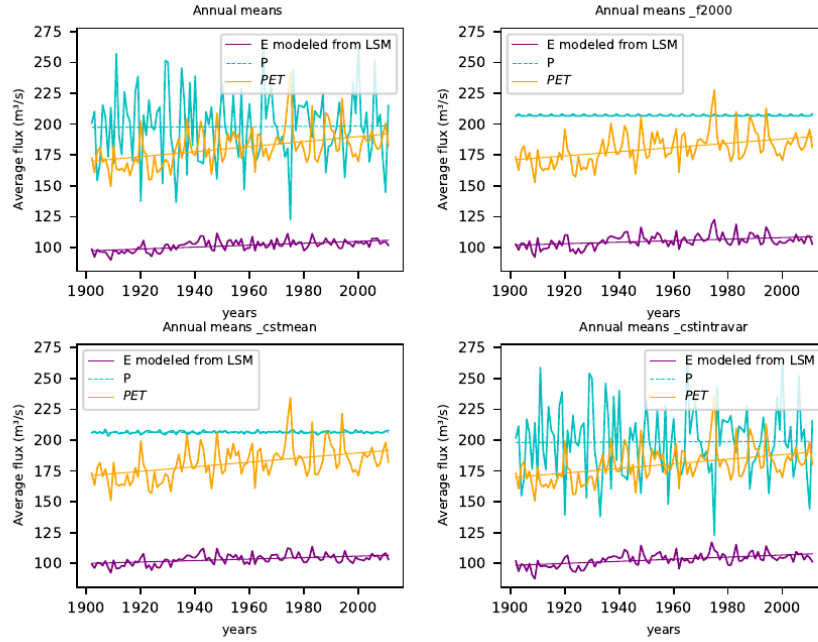
464 4.2 Comparing the effects of intra-annual variations of P on discharge 465 Q to the effects of variations in annual averages of P in Europe

466 We consider our area of study, Western Europe (2134 watersheds modeled) (fig. 7).
 467 We first look at the results for the reference forcing for two examples, a basin in Eng-
 468 land (fig. 5) and a basin in Italy (fig. 6). The discharge obtained through our method-
 469 ology applied to the reference forcing is the first plot on the top left fig. 5b and 6b. The
 470 blue curve represents the full discharge modeled $Q = f(C, \nu(t))$, the purple line the dis-
 471 charge $Q_c = f(C, \bar{\nu})$ with only variations in C accounted for and the black line $Q_\nu =$
 472 $f(C_{rand}, \nu(t))$ with only the variations of $\nu(t)$, mostly changes in the intra-annual co-
 473 variance of P and PET , accounted for. We represented anomaly of discharge $((Q - Q_{mean})/Q_{mean})$
 474 in order to better compare the plots to each other. For both examples (fig. 5b and 6b),
 475 with the reference forcing, the dominant effect in the variations of annual discharge Q
 476 (blue line) is due to the annual mean of climate variables C (purple line). Indeed, the
 477 blue and the purple curves have very similar variations and trends. We extend the re-
 478 sults over all of Europe. Fig. 7a, 7b, 7c show the relative trends over each basins, respec-
 479 tively of Q , Q_c and Q_ν , for the reference forcing. There are significant decreases in the
 480 total discharge Q (fig. 7a) (-0.3% to -0.4% per year over the past century) over sparse
 481 basins in Spain, the Pyrenees, Italy, Slovenia, Greece and Eastern Europe. There are sig-
 482 nificant increases (fig. 7a) (+0.2% to +0.4% per year over the past century) over sparse
 483 basins in France, Germany, Denmark, Sweden, Northern UK and Serbia. Similarly as
 484 for the two examples, these trends are mostly due to changes in the annual averages of



Trent, River : Colwick

(a) Annual average of climate variables P (light blue line), PET (yellow line) and E (purple line) modeled with the LSM for each academic forcing. Not shown here, the intra-annual distribution of P has been fixed for the forcings f_{2000} and $cstintravar$.



(b) Normalized anomaly of discharge estimated with Budyko: $Q = f(P, PET, \nu(t))$ (blue line), $Q_c = f(P, PET, \bar{\nu})$ (purple line), $Q_v = f(P_{rand}, PET_{rand}, \nu(t))$ (black line) with their associated trends. Unsignificant trends are dashed. Here the results for each academic forcing are shown. The scale of the y-axis changes and is divided by 5 for the forcings f_{2000} and $cstmean$.

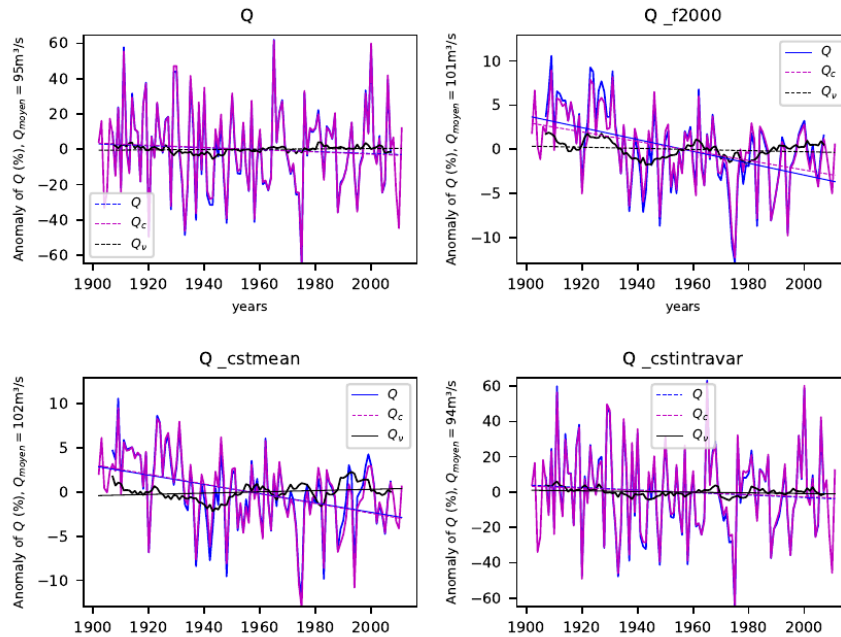
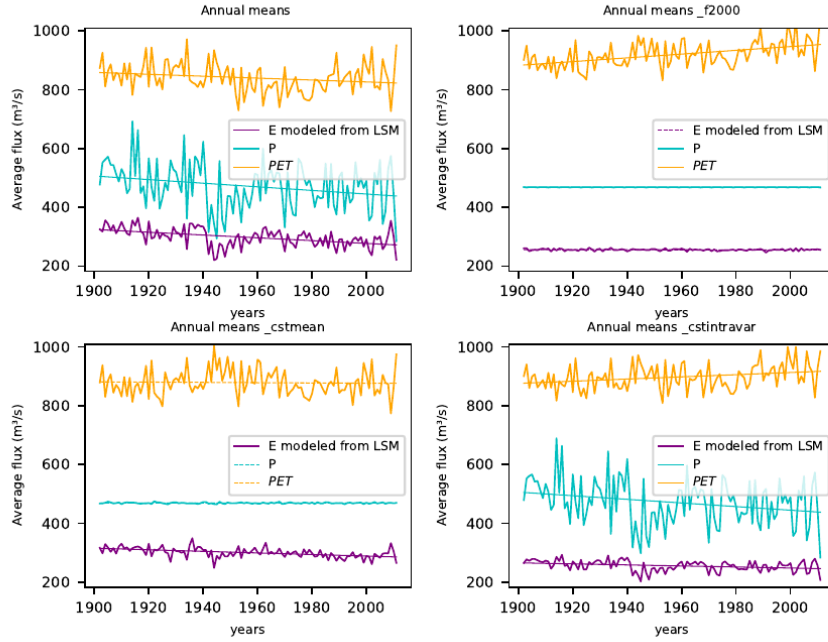


Figure 5. Example 1: Time series obtained through the full application of our methodology for a given basin in England.



Tiber River : Roma

(a) Annual average of climate variables P (light blue line), PET (yellow line) and E (purple line) modeled with the LSM for each academic forcing. Not shown here, the intra-annual distribution of P has been fixed for the forcings f_{2000} and $cstintravar$.



(b) Normalized anomaly of discharge estimated with Budyko: $Q = f(P, PET, \nu(t))$ (blue line), $Q_c = f(P, PET, \bar{\nu})$ (purple line), $Q_\nu = f(P_{rand}, PET_{rand}, \nu(t))$ (black line) with their associated trends. Unsignificant trends are dashed. Here the results for each academic forcing are shown. The scale of the y-axis changes and is divided by 5 for the forcings f_{2000} and $cstmean$.

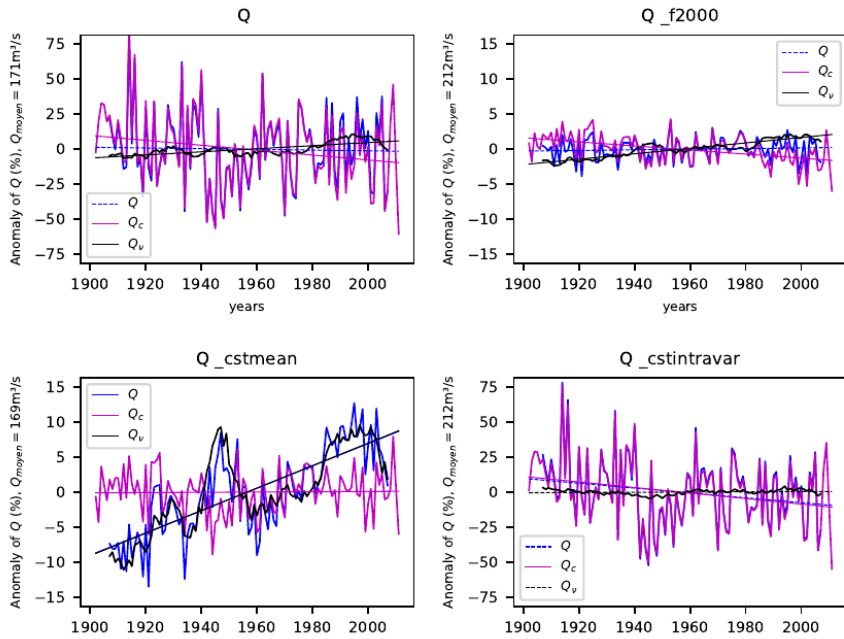


Figure 6. Example 2: Time series obtained through the full application of our methodology for a given basin in Italy.

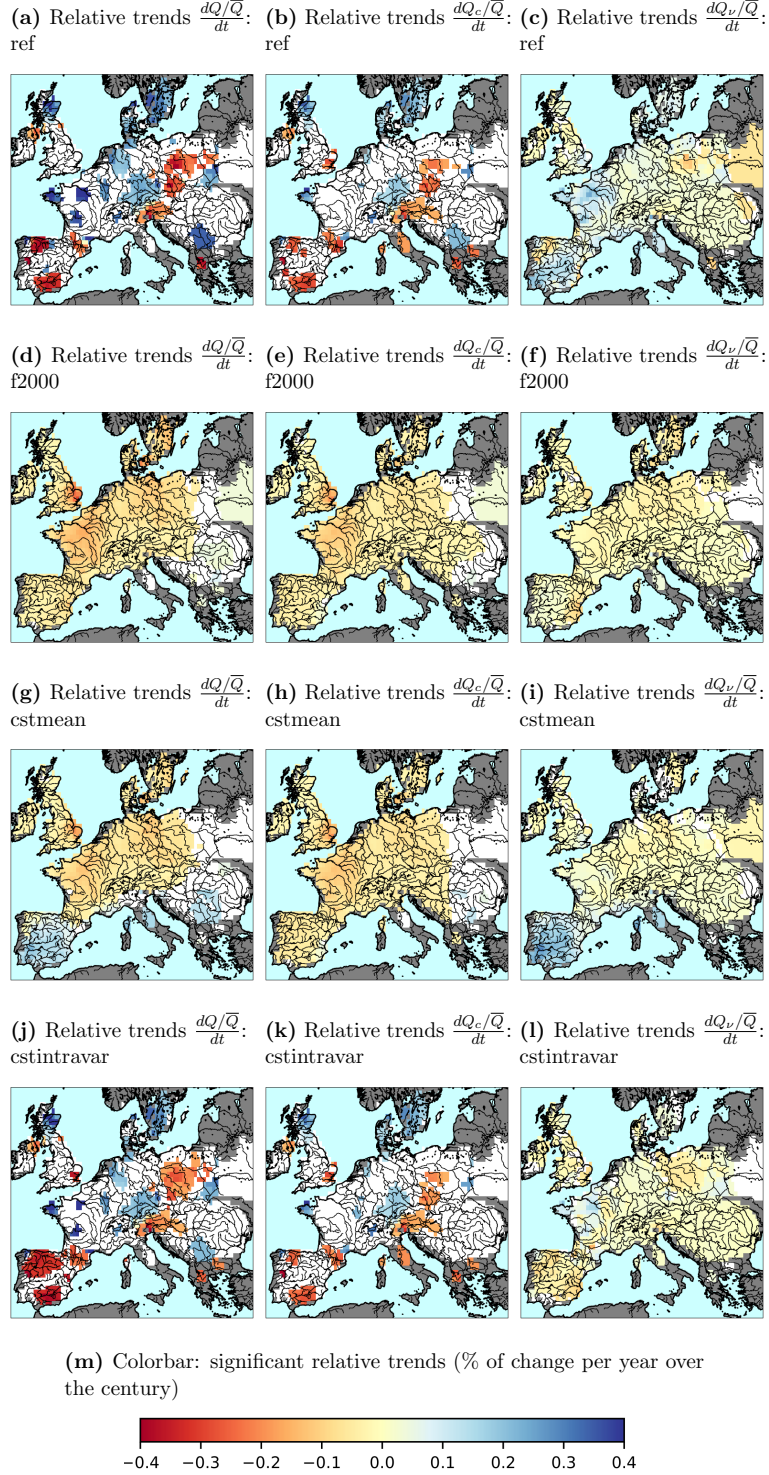


Figure 7. Decomposition of significant relative Q trends (% of change per year over the century) for all the tested forcings: the first line is the reference forcing. The first column is the total change in Q , the second column is the partial change due to trends in annual average of P and PET , the last column is the partial change due to changes in the watershed parameter, mostly due to trends in intra-annual distribution of P and PET . For the modified forcings: $f2000$ has the annual average and intra-annual distribution of P fixed for every year to their value for the year 2000. $cstmean$ has only the annual average of P fixed. $cstintravar$ has only the intra-annual distribution of P fixed. White areas don't have significant trends.

485 $C = (P, PET)$ since the Budyko framework with a constant parameter Q_c captures most
 486 of it (fig 7b). The inter-annual variability of C is high, making the trends less than 95%
 487 significant over most basins for Q and Q_c . Changes in C are the dominant factors ex-
 488 plaining the trends in Q over the past century in Europe. This is confirmed by the re-
 489 sults obtained with the forcing *cstintravar* (bottom right for fig. 5b and 6b and maps
 490 fig. 7j to 7l). It shows that without inter-annual changes in P distribution, in other words,
 491 with a maximum reduction of the inter-annual changes in the annual covariance of P and
 492 PET , the discharge Q obtained and the associated relative trends are very similar to the
 493 results obtained with the reference forcing. Therefore the effects of changes in the co-
 494 variance of P and PET is minor compared to the effects of changes in the annual mean
 495 of climate variables C in most of Europe.

496 However, there are some areas where the effects of intra-annual distribution of P
 497 can't be neglected. If we look at the Tiber river in Italy (fig. 6b), the trend in Q_c is sim-
 498 ilarly significant for both the reference forcing and the forcing *cstintravar* but the trend
 499 in the total discharge Q is only significant for the forcing *cstintravar*. For the reference
 500 forcing, the decreasing trend in the discharge due to C (Q_c) is counteracted by the in-
 501 creasing trend due to $\nu(t)$ (Q_ν), making the final trend in discharge Q not significant.
 502 More generally over Europe, when we erase the inter-annual variability of C , we capture
 503 the effect of trends in the intra-annual distribution of P and PET , through our $\nu(t)$, in
 504 Q_ν (fig 7c). It tends to increase discharge especially in the South-West of Spain, Italy
 505 and Western France (+0.1% per year over the century). It corresponds to the increas-
 506 ing trend for the black line in fig. 6b, top left graphs for the Tiber river. It has an op-
 507 posite trend towards decreasing discharge in Eastern Europe and has a rather neutral
 508 effect in the rest of Europe (fig. 7c and example of the basin in England fig. 5b, top left
 509 graph, black line). This effect is masked in the total trend in discharge by the high inter-
 510 annual variability of C (fig. 5b and 6b, top left graphs, blue line). However it amplifies
 511 the trends due to changes in annual averages of C over some watersheds such as the Duero
 512 basin (North-West of Spain, decrease in discharge), western France and northern Ger-
 513 many (significant increase in discharge over some watersheds where the effect of changes
 514 in C alone was not significant). In some other areas, such as for the Tiber river in Italy,
 515 or in Southern UK, the effect of intra-annual variability of P and PET counteracts the
 516 effect of C , making the relative total Q trends loose their significance due to opposite
 517 signals (decreasing trend due to the evolution of C while the effect of change in the intra-
 518 annual distribution of the climate variables tend to an increase in the discharge).

519 To look more closely at the effects of the intra-annual variations of P on discharge,
 520 we examine the results for the synthetic forcing *f2000* and *cstmean* (respectively top right
 521 and bottom left fig. 5b and 6b and maps 7d to 7f and 7g to 7i).

522 When we look at the results for the synthetic forcing *f2000* (fig 7d to 7f), for which
 523 P has been entirely set to that of year 2000 for each year, we therefore only get the trends
 524 due to changes in PET . For the synthetic forcing *cstmean*, only the annual mean of P
 525 has been set, we therefore get the trends due to PET and due to changes in the intra-
 526 annual distribution of P .

527 Free of the high inter-annual variability of the annual mean of P , the trends in dis-
 528 charge are significant over more watersheds for both forcings, with significant trends for
 529 1883 basins with the forcing *f2000* and 1756 basins for the forcing *cstmean* against only
 530 352 basins with significant trends in Q out of 2134 for the reference forcing. However,
 531 their magnitude is also a lot smaller. When we compare to the discharge obtained with
 532 the reference forcing, it shows that the main factor driving Q is the annual mean of P
 533 since when free of its variations, the discharge looks completely different.

534 For the forcing *f2000*, the effect of PET is towards a decrease in discharge over all
 535 of Europe (less than -0.1% to -0.2% per year over the century) (fig. 7d). It is found for
 536 both the chosen examples that the effect of PET (top right graphs) tends to decrease

537 discharge (purple line, Q_c when P has been fixed). It is coherent with the the signifi-
 538 cant increase in PET (fig. 5a and 6a, top right). The effect of intra-annual variations
 539 of PET (fig 7f and black lines, top right graph fig. 5b and 6b) has the same order of mag-
 540 nitude, if not a little smaller (less than -0.1% per year over the century), than the effect
 541 of inter-annual change of the annual average of PET (fig 7e or purple line top right graph
 542 fig. 5b and 6b). It tends to amplify the effect of the later, especially over Western France
 543 and Southern UK and has a slight opposite effect towards increasing trends in Q (less
 544 than $+0.08\%$ per year over the century) over the East of Europe, West of Spain and for
 545 the Tiber river. The effect of changes in annual mean of PET in this specific case is can-
 546 celed in the total discharge (blue line) by the effect of the changes in the intra-annual
 547 distribution of PET captured in Q_ν (black line) (6b).

548 For the forcing $cstmean$, we now add the effect of changes in the covariance of P
 549 and PET due to changes in the intra-annual distribution of P . Depending on the area,
 550 there are two different responses. The two basins chosen in example each correspond to
 551 one type of response. In the case of the basin in England (Trent river), the results ob-
 552 tained for the forcing $cstmean$ (fig. 5b, bottom left) are very similar to the results ob-
 553 tained for $f2000$ (fig.5b, top right). It means that the effect due to changes in the co-
 554 variance of P and PET have little impact compare to the effect of the annual mean of
 555 PET over that basin. It matches the results over the North of Europe, especially over
 556 France, Germany, South of UK where the trends in Q (fig 7g) are mostly driven by changes
 557 in the annual mean of PET (fig 7h). However over the second example of the Tiber river
 558 in Italy, the results obtained for the forcing $cstmean$ (fig. 6b, bottom left) shows that
 559 the changes in the total discharge Q (blue line) match the changes due to the evolution
 560 of $\nu(t)$ (Q_ν , black line). In that latter case, the effect of the intra-annual variations of
 561 P is dominant to the effect of changes in PET . This matches the results over the South
 562 of Europe (Spain, Italy) where for the forcing $cstmean$, the trends in Q (fig 7g) are mostly
 563 driven by changes in $\nu(t)$ (fig 7i). These trends are increasing trends in discharge which
 564 diverges from the trends due to changes in C in the area (reference forcing and forcing
 565 $f2000$, purple lines).

566 To sum up the results obtained with the synthetic forcings, the annual mean of P
 567 is the first driver of change in the annual discharge over all of Europe but its high inter-
 568 annual variability tends to hide the trends over most areas. The second most important
 569 climatic driver of change in discharge is dependent on the area. Over the South of Eu-
 570 rope (Italy, Spain) where water is the limiting factor to evapotranspiration, the second
 571 most important climatic factor driving discharge changes is the intra-annual distribu-
 572 tion of P . Over the rest of Europe where water is less limiting, the second most impor-
 573 tant factor driving discharge changes is the increasing PET .

574 5 Discussion

575 Several studies have shown the impact of climate change on climate variables over
 576 the past century on our area of interest. Annual precipitations increased between 1901
 577 and 2005 over most of Europe but the Mediterranean area where they tend to decrease
 578 (Douville et al., 2021; Knutson & Zeng, 2018). Trends per decade are less significant due
 579 to the high inter-annual variability of P (Douville et al., 2021). Trends in PET are linked
 580 to an increase in the energy available at the surface, highly correlated to the raising tem-
 581 peratures (Douville et al., 2021; Vicente-Serrano et al., 2014). Few studies have directly
 582 looked at the trends in PET over Europe, except over the Mediterranean area where stud-
 583 ies have shown a significant increase in PET over the end of the century (Vicente-Serrano
 584 et al., 2014; Kitsara et al., 2013). The intra-annual variations of climatic variables are
 585 more difficult to assess and very little indices exist to measure the inter-annual changes
 586 in the distribution of climate variables. García-Barrón et al. (2018) defined indices to
 587 assess the evolution over time of the intra-annual cycle of P over the Iberian peninsula.
 588 They find that there is a shift over the end of the century of the main rainfall periods

589 towards autumn, especially over the Atlantic basins and an increase in the inter-annual
590 variability of the intra-annual cycle, especially over the Mediterranean basins.

591 We look at the trends in P , PET and calculated the indices defined by García-Barrón
592 et al. (2013) to evaluate the trends in the intra-annual cycle of P for the forcing GSWP3.
593 We find that our results concur with those in the literature, validating that this forcing
594 reasonably reproduces the climatic trends of the past century over Europe. The trends
595 in PET are significantly (95% level) increasing over all of Europe. However the trends
596 in P are most often non significant because of its high inter-annual variability, with a
597 significant trend in the annual average of P for 413 catchments out of the 2134 selected.
598 The trends in the intra-annual cycle are also mostly qualitative.

599 We find in the present study that the main driver of annual discharge Q is the an-
600 nual mean of P . As expected with the increase in P over western Europe and the de-
601 crease in P observed in the Mediterranean area, the trends in Q have a concurring di-
602 rection.

603 Our methodology allows to separate the effect of this main driver from secondary
604 climatic parameter which also affect discharge trends. The effects of intra-annual vari-
605 ations of P on discharge are mostly considered in the literature through the study of sea-
606 sonality and annual extremes of P and PET , to examine their impact on floods (Douville
607 et al., 2021; Rottler et al., 2020; Milly et al., 2002) and drought events (Douville et al.,
608 2021; Vicente-Serrano et al., 2014). However we find that over the Iberian peninsula and
609 the Mediterranean area at least, the effect of the evolution of intra-annual variations of
610 P is the second most important factor impacting the changes in the annual discharge,
611 with a higher effect on discharge than the increase of PET over the century. The intra-
612 annual covariance of P and PET impacts the annual behavior of the catchment and the
613 annual balance between evapotranspiration and discharge since it changes the timing be-
614 tween water and energy availability throughout the year. Therefore intra-annual distri-
615 bution of P deserves more attention when studying the evolution of annual discharge.
616 The evolution of the intra-annual cycle of P tends towards decreasing discharge in the
617 Mediterranean area. It counteracts partially the effect of decreasing P and increasing
618 PET on discharge. It could be explained by the tendencies of the annual cycle to have
619 an increasingly marked seasonality, concentrating rain events in less but more intense
620 events over the year and thus increasing runoff and relative discharge. Furthermore, our
621 methodology allows to identify these effects despite the only qualitative trends observed
622 in the indices used to measure the intra-annual distribution of P .

623 Over the rest of Europe where water is less of a limiting factor, the secondary most
624 important climatic factor on discharge changes is PET , which leads to a decrease in dis-
625 charge due to the increasing evaporative demand by the atmosphere. In the Mediterranean
626 area, PET trends have a lesser impact because the water limit is dominating, being al-
627 ready reached at the end of spring and during all summer. A warmer summer doesn't
628 have therefore a strong impact.

629 **6 Conclusions and perspectives**

630 Similarly to the results of Abatzoglou and Ficklin (2017); S. Li et al. (2022); Xing
631 et al. (2018), we found that the original Budyko framework with a constant watershed
632 parameter $\bar{\nu}$ does not capture climate related changes in the watershed behavior impact-
633 ing its evaporation efficiency. We have shown that this could be alleviated by introduc-
634 ing a time-dependent parameter $\nu(t)$ which would include the effect of these changes.

635 Our method doesn't need to define an expression of this $\nu(t)$, which would be highly
636 dependent on the area of study and on the factors available. It can directly be used to
637 estimate the effects over time of changes in the climatic parameter and quantify their
638 relative impacts on discharge trends. To do so we use a time-moving window. The choice

of the window size determines the size of the trends accounted for. It works as a filter of frequency and only captures the effect of variations over periods the size of the window or larger. We had to find a balance between the length of our dataset and the pertinent length of the trends we wanted to analyse. Since we want to look at the effects of climate change, we do not need to capture the high inter-annual variability and can focus on decadal trends or longer. Furthermore, a shorter time window would not be adapted to the hypothesis to the Budyko framework which needs a long enough time-period to be fitted. So the window can't be shorter (Tian et al., 2018). We could test longer time-window to test which is the limit time-length capturing the most impacting effect on discharge. However the longer the time-window, the fewer the points we will have to evaluate the trends.

We apply our modified Budyko framework to LSM outputs to isolate the discharge variations due to changes in climate factors. This methodology relies on the capacity of the chosen LSM to reproduce the "natural" response of a catchment to climate, such as its behavior and response to changes in the intra-annual distribution of P . Our methodology to calculate a time-varying $\nu(t)$ for the Budyko framework, when applied to the output of LSM simulated watersheds with constant hydrological properties, allows to capture the long-term variability of Q due to climate effects not included in the variations of the averages of P and PET .

These changes captured in the time varying $\nu(t)$ are mostly due to changes in the covariance of the intra-annual distribution of P and PET . However the effect of intra-annual distribution of climate variables on discharge is not completely independent from the annual mean of P and PET which can impact the magnitude of the identified trends. This is shown by the slight differences observed in Q_ν between respectively the reference forcing and the forcing *csmean* (fig. 7c and 7i) and between the forcing *f2000* and the forcing *csintravar* (fig. 7f and 7l). For each pair of forcings, the intra-annual distribution of P is the same but the inter-annual mean of P differs between the two. The difference observed in Q_ν for each pairing is due to a linked effect between the annual mean and the intra-annual distribution of P . Therefore the amplitude of the effect of intra-annual distribution of P and PET quantified here may depend on the choice of the average P fixed (P from the year 2000 in this study). However the differences are smaller than the identified trends, suggesting that the main conclusions over Europe would not change. When studying specific basins, it could be however interesting to choose specific pairings intra-annual distributions/annual averages of P to construct synthetic forcings, to compare how specific associations combine. When looking at absolute values instead of trends, the choice of the reference year will also play an important part. For instance for the watershed in Italy, the effect of the intra-annual distribution of P of the year 2000 tend to a higher discharge (fig. 6b, bottom left, black line, the intra-annual distribution of the end of the century tend to a higher discharge), explaining that when we set every year to its value for the forcings *f2000* and *csintravar*, we get a higher average discharge over the entire century (see average discharge, y-axis legend).

Furthermore, we could not simply fix PET or its intra-annual variations in our synthetic forcings due to its non linearity dependence on a number of climate variables. Therefore we could not decompose the effects of PET as easily as for the effects of P , which would be interesting to do especially in the areas where P is less limiting such as in the West of France or in the North of Europe.

The amplitude of the results could also depend on the choice of the model or of the forcing data. We tested the use of other forcing datasets: WFDEI (Weedon et al., 2014), which covers the time period from 1979 to 2010, with the same resolution than GSWP3 and E2OFD (Beck et al., 2017), also covering 1979 to 2010 but at a lower resolution. We also tested the use of another model with another forcing, the model SURFEX (Quintana-Seguí et al., 2020) forced with SAFRAN (Quintana-Seguí et al., 2017), over the Ebro river. It gave very similar results over the overlapping period, with little differences in the sig-

692 nificance of the trends and their amplitude, showing that the results mostly are depen-
693 dent on the resolution of the forcing rather than on the forcing or the model used. This
694 validates our methodology to use a LSM as a climatic reference. Again when looking at
695 specific basins, it would be interesting to use higher resolution forcings to get a more ac-
696 curate picture on the effects of climate change on discharge. We could detail the diver-
697 sity of behaviors between sub-basins within a given catchment, for instance separating
698 the behavior of upstream sub-basins within mountainous areas from the downstream part
699 of the catchment which could be differently responding to climate change.

700 If we were to work from observations instead of model outputs, there would be other
701 non-climate related sources of variability such as direct human activities or vegetation
702 changes which would modify the watersheds' behaviors. Our next step is to apply the
703 methodology to quantify these human induced changes and compare their magnitude
704 to those attributed to climate in the present study responses.

705 **7 Open Research**

706 **Data availability statement**

707 The forcing dataset GSWP3 used to grid P and other climate data and run the LSM
708 over Europe between 1901 and 2010 in the study is attributed to Hyungjun (2017). It
709 is available upon request via doi:10.20783/DIAS.501.

710 The Land Surface Model used to calculate $E0$ and model the discharge in this study
711 is the LSM Organizing Carbon and Hydrology In Dynamic Ecosystems (ORCHIDEE)
712 from the Institut Pierre Simon Laplace (IPSL). The Main version used in this study is
713 available upon request on the official website <https://orchidee.ipsl.fr/>.

714 It relies on the hydrological elevation model HydroSHEDS (Lehner et al., 2008) to
715 construct its routing graphs for rivers and reconstruct the upstream areas of gauging sta-
716 tions placed on its grid. It is available to download from <https://www.hydrosheds.org/>.

717 The gauging stations positioned on the grid come from a database composed from
718 several sources. The main dataset is the one from the Global Runoff Data Centre (GRDC).
719 It is available to download from [https://www.bafg.de/GRDC/EN/02_srvcs/21_tmsrs/
720 riverdischarge_node.html](https://www.bafg.de/GRDC/EN/02_srvcs/21_tmsrs/riverdischarge_node.html). It was completed over Spain with data obtained from the
721 Geoportail of Spain Ministerio (Ministerio de Agricultura, pesca y alimentacion, Minis-
722 terio para la transicion ecologica y el reto demografico, 2020) and over France with data
723 from the database HYDRO (Ministere de l'ecologie, du developpement durable et de l'energie)
724 (available on request to <https://www.hydro.eafrance.fr/>, downloaded in February
725 2021). In this study, we only used the position of these stations and the associated up-
726 stream area to reconstruct meaningful watersheds.

References

- Abatzoglou, J. T., & Ficklin, D. L. (2017, September). Climatic and physiographic controls of spatial variability in surface water balance over the contiguous United States using the Budyko relationship. *Water Resources Research*, *53*, 7630–7643. doi: 10.1002/2017WR020843
- Andréassian, V., & Sari, T. (2019, May). Technical Note: On the puzzling similarity of two water balance formulas – Turc–Mezentsev vs. Tixeront–Fu. *Hydrology and Earth System Sciences*, *23*(5), 2339–2350. doi: 10.5194/hess-23-2339-2019
- Barella-Ortiz, A., Polcher, J., Tuzet, A., & Laval, K. (2013, November). Potential evaporation estimation through an unstressed surface-energy balance and its sensitivity to climate change. *Hydrology and Earth System Sciences*, *17*(11), 4625–4639. doi: 10.5194/hess-17-4625-2013
- Beck, H. E., van Dijk, A. I. J. M., Levizzani, V., Schellekens, J., Miralles, D. G., Martens, B., & de Roo, A. (2017, January). MSWEP: 3-hourly 0.25°° global gridded precipitation (1979–2015) by merging gauge, satellite, and reanalysis data. *Hydrology and Earth System Sciences*, *21*(1), 589–615. doi: 10.5194/hess-21-589-2017
- Christidis, N., & Stott, P. A. (2022, August). Human Influence on Seasonal Precipitation in Europe. *Journal of Climate*, *35*(15), 5215–5231. doi: 10.1175/JCLI-D-21-0637.1
- Douville, H., Raghavan, K., Renwick, J., Allan, R., Arias, P., Barlow, M., . . . Zolina, O. (2021). Water Cycle Changes. In *Climate Change 2021: The Physical Science Basis. Contribution of Working Group I to the Sixth Assessment Report of the Intergovernmental Panel on Climate Change.*, 1055–1210. doi: 10.1017/9781009157896.010
- du, C., Sun, F., Yu, J., Liu, X., & Yaning, C. (2016, January). New interpretation of the role of water balance in an extended Budyko hypothesis in arid regions. *Hydrology and Earth System Sciences*, *20*, 393–409. doi: 10.5194/hess-20-393-2016
- García-Barrón, L., Aguilar-Alba, M., Morales, J., & Sousa, A. (2018). Intra-annual rainfall variability in the Spanish hydrographic basins. *International Journal of Climatology*, *38*(5), 2215–2229. doi: 10.1002/joc.5328
- García-Barrón, L., Morales, J., & Sousa, A. (2013, November). Characterisation of the intra-annual rainfall and its evolution (1837–2010) in the southwest of the Iberian Peninsula. *Theoretical and Applied Climatology*, *114*(3), 445–457. doi: 10.1007/s00704-013-0855-7
- Gentine, P., D’Odorico, P., Lintner, B., Sivandran, G., & Salvucci, G. (2012, October). Interdependence of climate, soil, and vegetation as constrained by the Budyko curve. *Geophysical Research Letters*, *39*, 19404. doi: 10.1029/2012GL053492
- Hyungjun, K. (2017). Global Soil Wetness Project Phase 3 Atmospheric Boundary Conditions (Experiment 1) [dataset]. *Data Integration and Analysis System (DIAS)*, *5*. doi:10.20783/DIAS.501
- Jiang, C., Xiong, L., Wang, D., Liu, P., Guo, S., & Xu, C.-Y. (2015, March). Separating the impacts of climate change and human activities on runoff using the Budyko-type equations with time-varying parameters. *Journal of Hydrology*, *522*, 326–338. doi: 10.1016/j.jhydrol.2014.12.060
- Kitsara, G., Papaioannou, G., Papathanasiou, A., & Retalis, A. (2013, April). Dimming/brightening in Athens: Trends in Sunshine Duration, Cloud Cover and Reference Evapotranspiration. *Water Resources Management*, *27*(6), 1623–1633. doi: 10.1007/s11269-012-0229-4
- Knutson, T. R., & Zeng, F. (2018, June). Model Assessment of Observed Precipitation Trends over Land Regions: Detectable Human Influences and Possible Low Bias in Model Trends. *Journal of Climate*, *31*(12), 4617–4637. doi:

- 10.1175/JCLI-D-17-0672.1
- 782
783 Lehner, B., Verdin, K., & Jarvis, A. (2008). New Global Hydrography Derived From
784 Spaceborne Elevation Data [dataset]. *Eos, Transactions American Geophysical*
785 *Union*, 89(10), 93–94. doi: 10.1029/2008EO100001
- 786 Li, D., Pan, M., Cong, Z., Zhang, L., & Wood, E. (2013). Vegetation control on
787 water and energy balance within the Budyko framework. *Water Resources Re-*
788 *search*, 49(2), 969–976. doi: 10.1002/wrcr.20107
- 789 Li, S., Du, T., & Gippel, C. J. (2022, March). A Modified Fu (1981) Equation
790 with a Time-varying Parameter that Improves Estimates of Inter-annual Vari-
791 ability in Catchment Water Balance. *Water Resources Management*, 36(5),
792 1645–1659. doi: 10.1007/s11269-021-03057-1
- 793 Luo, Y., Yang, Y., Yang, D., & Zhang, S. (2020, November). Quantifying the impact
794 of vegetation changes on global terrestrial runoff using the Budyko framework.
795 *Journal of Hydrology*, 590, 125389. doi: 10.1016/j.jhydrol.2020.125389
- 796 Milly, P. C. D., Dunne, K. A., & Vecchia, A. V. (2005, November). Global pat-
797 tern of trends in streamflow and water availability in a changing climate. *Na-*
798 *ture*, 438(7066), 347–350. doi: 10.1038/nature04312
- 799 Milly, P. C. D., Wetherald, R. T., Dunne, K. A., & Delworth, T. L. (2002, January).
800 Increasing risk of great floods in a changing climate. *Nature*, 415(6871), 514–
801 517. doi: 10.1038/415514a
- 802 Moriasi, D. N., Arnold, J. G., Liew, M. W. V., Bingner, R. L., Harmel, R. D., &
803 Veith, T. L. (2007). MODEL EVALUATION GUIDELINES FOR SYSTEM-
804 ATIC QUANTIFICATION OF ACCURACY IN WATERSHED SIMULA-
805 TIONS. *TRANSACTIONS OF THE ASABE*, 50, 16.
- 806 Ning, T., Zhou, S., Chang, F., Shen, H., Li, Z., & Liu, W. (2019, September). Inter-
807 action of vegetation, climate and topography on evapotranspiration modelling
808 at different time scales within the Budyko framework. *Agricultural and Forest*
809 *Meteorology*, 275, 59–68. doi: 10.1016/j.agrformet.2019.05.001
- 810 Polcher, J., Schrapffer, A., Dupont, E., Rinchuso, L., Zhou, X., Boucher, O., ...
811 Servonnat, J. (2022, September). Hydrological modelling on atmospheric grids;
812 using graphs of sub-grid elements to transport energy and water. *EGUsphere*,
813 1–34. doi: 10.5194/egusphere-2022-690
- 814 Quintana-Seguí, P., Barella-Ortiz, A., Regueiro-Sanfiz, S., & Miguez-Macho, G.
815 (2020, May). The Utility of Land-Surface Model Simulations to Provide
816 Drought Information in a Water Management Context Using Global and Lo-
817 cal Forcing Datasets. *Water Resources Management*, 34(7), 2135–2156. doi:
818 10.1007/s11269-018-2160-9
- 819 Quintana-Seguí, P., Turco, M., Herrera, S., & Miguez-Macho, G. (2017, April).
820 Validation of a new SAFRAN-based gridded precipitation product for Spain
821 and comparisons to Spain02 and ERA-Interim. *Hydrology and Earth System*
822 *Sciences*, 21(4), 2187–2201. doi: 10.5194/hess-21-2187-2017
- 823 Roderick, M. L., & Farquhar, G. D. (2011). A simple framework for relating vari-
824 ations in runoff to variations in climatic conditions and catchment properties.
825 *Water Resources Research*, 47(12). doi: 10.1029/2010WR009826
- 826 Rottler, E., Francke, T., Bürger, G., & Bronstert, A. (2020, April). Long-
827 term changes in central European river discharge for 1869–2016: Impact of
828 changing snow covers, reservoir constructions and an intensified hydrolog-
829 ical cycle. *Hydrology and Earth System Sciences*, 24(4), 1721–1740. doi:
830 10.5194/hess-24-1721-2020
- 831 Simons, G. W. H., Bastiaanssen, W. G. M., Cheema, M. J. M., Ahmad, B., & Im-
832 merzeel, W. W. (2020, June). A novel method to quantify consumed fractions
833 and non-consumptive use of irrigation water: Application to the Indus Basin
834 Irrigation System of Pakistan. *Agricultural Water Management*, 236, 106174.
835 doi: 10.1016/j.agwat.2020.106174
- 836 Tian, L., Jin, J., Wu, P., & Niu, G.-y. (2018, December). Quantifying the Im-

- 837 pact of Climate Change and Human Activities on Streamflow in a Semi-Arid
 838 Watershed with the Budyko Equation Incorporating Dynamic Vegetation
 839 Information. *Water*, 10(12), 1781. doi: 10.3390/w10121781
- 840 Tuel, A., Schaeffli, B., Zscheischler, J., & Martius, O. (2022, May). On the links
 841 between sub-seasonal clustering of extreme precipitation and high discharge
 842 in Switzerland and Europe. *Hydrology and Earth System Sciences*, 26(10),
 843 2649–2669. doi: 10.5194/hess-26-2649-2022
- 844 Vicente-Serrano, S. M., Lopez-Moreno, J.-I., Beguería, S., Lorenzo-Lacruz, J.,
 845 Sanchez-Lorenzo, A., García-Ruiz, J. M., ... Espejo, F. (2014, April).
 846 Evidence of increasing drought severity caused by temperature rise in
 847 southern Europe. *Environmental Research Letters*, 9(4), 044001. doi:
 848 10.1088/1748-9326/9/4/044001
- 849 Wang, W., Zhang, Y., & Tang, Q. (2020, December). Impact assessment of climate
 850 change and human activities on streamflow signatures in the Yellow River
 851 Basin using the Budyko hypothesis and derived differential equation. *Journal*
 852 *of Hydrology*, 591, 125460. doi: 10.1016/j.jhydrol.2020.125460
- 853 Weedon, G. P., Balsamo, G., Bellouin, N., Gomes, S., Best, M. J., & Viterbo, P.
 854 (2014). The WFDEI meteorological forcing data set: WATCH Forcing Data
 855 methodology applied to ERA-Interim reanalysis data. *Water Resources Re-*
 856 *search*, 50(9), 7505–7514. doi: 10.1002/2014WR015638
- 857 Xing, W., Wang, W., Shao, Q., & Yong, B. (2018, January). Identification of dom-
 858 inant interactions between climatic seasonality, catchment characteristics and
 859 agricultural activities on Budyko-type equation parameter estimation. *Journal*
 860 *of Hydrology*, 556, 585–599. doi: 10.1016/j.jhydrol.2017.11.048
- 861 Xiong, M., Huang, C.-S., & Yang, T. (2020, June). Assessing the Impacts of Climate
 862 Change and Land Use/Cover Change on Runoff Based on Improved Budyko
 863 Framework Models Considering Arbitrary Partition of the Impacts. *Water*,
 864 12(6), 1612. doi: 10.3390/w12061612
- 865 Yang, D., Sun, F., Liu, Z., Cong, Z., Ni, G., & Lei, Z. (2007, April). Analyzing
 866 spatial and temporal variability of annual water-energy balance in nonhumid
 867 regions of China using the Budyko hypothesis. *Water Resources Research*,
 868 43(4). doi: 10.1029/2006WR005224
- 869 Zhang, L., Potter, N., Hickel, K., Zhang, Y., & Shao, Q. (2008, October). Water
 870 balance modeling over variable time scales based on the Budyko framework –
 871 Model development and testing. *Journal of Hydrology*, 360(1), 117–131. doi:
 872 10.1016/j.jhydrol.2008.07.021
- 873 Zhang, X., Dong, Q., Costa, V., & Wang, X. (2019, May). A hierarchical Bayesian
 874 model for decomposing the impacts of human activities and climate change on
 875 water resources in China. *Science of The Total Environment*, 665, 836–847.
 876 doi: 10.1016/j.scitotenv.2019.02.189
- 877 Zhao, J., Huang, S., Huang, Q., Wang, H., & Leng, G. (2018, September). De-
 878 tecting the Dominant Cause of Streamflow Decline in the Loess Plateau
 879 of China Based on the Latest Budyko Equation. *Water*, 10(9), 1277. doi:
 880 10.3390/w10091277
- 881 Zheng, Y., Huang, Y., Zhou, S., Wang, K., & Wang, G. (2018, December). Ef-
 882 fect partition of climate and catchment changes on runoff variation at the
 883 headwater region of the Yellow River based on the Budyko complemen-
 884 tary relationship. *Science of The Total Environment*, 643, 1166–1177. doi:
 885 10.1016/j.scitotenv.2018.06.195
- 886 Zveryaev, I. I. (2004). Seasonality in precipitation variability over Europe. *Journal*
 887 *of Geophysical Research: Atmospheres*, 109(D5). doi: 10.1029/2003JD003668